Research article

NMR IN BIOMEDICINE

Received: 26 June 2013, Revised: 6 March 2014, Accepted: 11 March 2014, Published online in Wiley Online Library

(wileyonlinelibrary.com) DOI: 10.1002/nbm.3110

Signal-to-noise ratio of a mouse brain ^{13}C CryoProbe™ system in comparison with room temperature coils: spectroscopic phantom and *in vivo* results

M. Sack[a,b]*, F. Wetterling[c,d], A. Sartorius[a,e], G. Ende[b] and W. Weber-Fahr[a,b]

MRI and MRS in small rodents demand very high sensitivity. Cryogenic transmit/receive radiofrequency probes (CryoProbes) designed for ^{1}H MRI of mouse brain provide an attractive option for increasing the performance of small-animal MR systems. As the Larmor frequency of ^{13}C nuclei is four times lower than that for ^{1}H nuclei, an even larger sensitivity improvement is expected for ^{13}C applications. The aim of this work was to evaluate the performance of a prototype ^{13}C CryoProbe™ for mouse brain MRS. To investigate the possible gain of the ^{13}C CryoProbe™, we acquired localized single-voxel ^{13}C spectra and chemical shift images of a dimethyl sulfoxide phantom with the CryoProbe™, as well as with two room temperature resonators. The cryogenically cooled resonator achieved approximately four-fold higher signal-to-noise ratio in phantom tests when compared with the best-performing room temperature coil. In addition, we present localized ^{13}C spectra of mouse brain obtained with the CryoProbe™, as well as with one of the room temperature coils, demonstrating the performance *in vivo*. In summary, the cryogenic cooling technique significantly enhances the ^{13}C signal sensitivity at 9.4 T and enables the investigation of metabolism within mouse brain. Copyright © 2014 John Wiley & Sons, Ltd.

Keywords: ^{13}C spectroscopy; CryoProbe™; SNR comparison; cryogenic coil; mouse; MRS

INTRODUCTION

MRS studies typically suffer from low signal-to-noise ratio (SNR), especially for ^{13}C MRS, owing to the low natural abundance (1.1%) of ^{13}C nuclei in living tissue and a gyromagnetic ratio which is four times lower than that for ^{1}H nuclei.

Dynamic ^{13}C MRS is a powerful tool for the investigation of brain metabolism *in vivo*. In conjunction with the administration of ^{13}C-enriched substrates, the ^{13}C label incorporation into different carbon positions of many important brain metabolites, i.e. glutamate and glutamine, can be measured (1,2). The use of an appropriate mathematical model then allows the computation of the metabolic flux rates of compartmentalized cerebral metabolism (3). Measurement of the time evolution of the glutamate and glutamine ^{13}C incorporation at the C4, C3 and C2 positions enables the differentiation between glial and neuronal compartments (4–7). Extending the mathematical model by a GABAergic (GABA, γ-aminobutyric acid) compartment requires the quantitative measurement of GABA. To our knowledge, there is only one publication presenting the dynamic quantitative measurement of GABA ^{13}C labeling in the *in vivo* murine brain using direct ^{13}C detection (2). This may be because of the low GABA concentration and thus the low SNR obtainable in a time resolution of a few minutes, even when GABA is enriched in ^{13}C.

To increase the SNR, cryogenic cooling has been suggested (8), as CryoProbes exploit the fact that there are noise sources which can be diminished directly. Noise arises from the sample, the coil and the preamplifier. Although the sample in *in vivo* experiments cannot be manipulated, the noise arising from the coil and preamplifier can be greatly reduced by lowering the operating temperature. Previous studies have reported an SNR improvement via cryogenic cooling for ^{1}H MRI of more than a factor of two in phantom and about 1.8–2.5 in *in vivo* murine

* *Correspondence to: M. Sack, Department of Neuroimaging/Translational Imaging, Central Institute of Mental Health, J5, 68159 Mannheim, Germany. E-mail: markus.sack@zi-mannheim.de*

a *M. Sack, A. Sartorius, W. Weber-Fahr*
Research Group Translational Imaging, Central Institute of Mental Health, Medical Faculty, Mannheim/Heidelberg University, Mannheim, Germany

b *M. Sack, G. Ende, W. Weber-Fahr*
Department of Neuroimaging, Central Institute of Mental Health, Medical Faculty, Mannheim/Heidelberg University, Mannheim, Germany

c *F. Wetterling*
Trinity College Institute of Neuroscience, the University of Dublin, Dublin, Ireland

d *F. Wetterling*
RF Methods and Imaging Group, Computer Assisted Clinical Medicine, Heidelberg University, Mannheim, Germany

e *A. Sartorius*
Department of Psychiatry and Psychotherapy, Central Institute of Mental Health, Medical Faculty, Mannheim/Heidelberg University, Mannheim, Germany

Abbreviations used: *Ala, alanine; BW, bandwidth; CSI, chemical shift imaging/image; CryoProbe™, cryogenic transmit/receive radiofrequency probe; DMSO, dimethyl sulfoxide; FWHM, full width at half-maximum; GABA, γ-aminobutyric acid; Gln, glutamine; Glu, glutamate; ISIS, image-selected in vivo spectroscopy; NAA, N-acetylaspartate; Q-factor, quality factor; RT, room temperature; SNR, signal-to-noise ratio.*

brain measurements at 200 MHz (9) and 400 MHz (10), respectively. Griffin *et al*. (11) expected an SNR gain of a factor of four for a ^{13}C CryoProbe™ for a 500-MHz NMR system.

The aim of this work was to evaluate the performance of a prototype ^{13}C CryoProbe™ system in comparison with room temperature coils: a commercially available, double-tuned, flat single-loop coil and an anatomically shaped home-built resonator which is close to the optimal design for the designated purposes. Special emphasis was given to the potentially available resonator solutions to conduct ^{13}C NMR and MRI measurements *in vivo*. Hence, the gain in SNR would not be solely attributed to cryogenic cooling of the coil and preamplifier, but also to the different resonator geometries allowed at room and cryo-temperatures. This includes a slightly different coil design of the CryoProbe™ compared with the home-built room temperature resonator and the use of a cooled narrow-band preamplifier which contributes to the SNR gain in the cryogenic receiver chain. However, as this is an essential part of the CryoProbe™ system, one should keep in mind that all results presented in this work describe the benefits of the cryo-technique, unless otherwise mentioned, rather than an exclusive cooling of the resonator's loop resistance. For this approach, we investigated the performance of the three coils by obtaining localized single-voxel spectra and three-dimensional chemical shift images (CSIs) in a phantom, and also compared the standard planar single-loop room temperature coil with the CryoProbe™ in an *in vivo* experiment.

THEORY

As described in refs. (8,9), the gain in SNR of a CryoProbe™ in comparison with a room temperature coil, neglecting the noise contributions from the respective preamplifiers, can be expressed as:

$$\mathrm{SNR}_{\mathrm{gain}} = \frac{\mathrm{SNR}_{\mathrm{cryo}}}{\mathrm{SNR}_{\mathrm{RT}}} = \frac{\sqrt{R_S T_S + R_{C,\mathrm{RT}} T_{C,\mathrm{RT}}}}{\sqrt{R_S T_S + R_{C,\mathrm{cryo}} T_{C,\mathrm{cryo}}}} \quad [1]$$

where R_S and $R_{C,X}$ are the resistances of the sample and coil, respectively, subscripts 'RT' and 'cryo' represent the room temperature coil and CryoProbe™, respectively, subscripts 'S' and 'C' denote the sample and coil, respectively, and T is the temperature. According to ref. (8), the resistance of the sample R_S can be approximated as follows:

$$R_S \approx \frac{2}{3\pi} \sigma {\mu_0}^2 \omega^2 n^2 a^3 \arctan\left(\frac{a\pi}{8d}\right) \quad [2]$$

where σ is the average conductivity of the sample, μ_0 is the magnetic permeability of free space, ω is the Larmor frequency, n is the number of turns, a is the coil radius and d is the distance between the coil and sample, and the resistance of the coil R_C is given by:

$$R_C = \sqrt{0.5 \rho_C \mu_0 \omega} \cdot n^2 \xi \frac{a}{r}, \quad [3]$$

where ρ_C is the electrical resistivity of the coil material (temperature dependent), r' is the wire radius and ξ is the proximity effect factor. As both resistances R_S and R_C are frequency dependent, there is also a frequency dependence of the expected gain in SNR, which increases with decreasing frequency. Therefore, particularly for X-nuclei, which have a lower gyromagnetic ratio than protons, the achievable gain in SNR can be higher under the same experimental set-up (same sample and coil dimensions). As the CryoProbe™ used operates at a very low coil temperature, together with the reduced coil resistance, the total coil noise contribution $R_{C,\mathrm{cryo}} \times T_{C,\mathrm{cryo}}$ is very low and the SNR moves close to the sample limit, i.e. most of the noise originates from the sample. As this is expected to hold true for both ^{1}H and ^{13}C frequencies, it allows for a simple estimate of the expected SNR gain for ^{13}C CryoProbes relative to ^{1}H CryoProbes (for the same B_0 field and coil geometry). Under the assumption of the following parameters, $a = 0.01$ m, $d = 0.001$ m, $\sigma = 0.66$ S/m, $\xi a/r = 40$ (12), $T_S = 310$ K, $T_{C,\mathrm{RT}} = 293$ K and $T_{C,\mathrm{cryo}} = 0$ K (representing zero cryogenic coil noise), the SNR gain at 100 MHz (the carbon frequency at 9.4 T) compared with that at 400 MHz (the proton frequency at 9.4 T) leads to:

$$\frac{\mathrm{SNR}_{\mathrm{gain,cryo}}(100\ \mathrm{MHz})}{\mathrm{SNR}_{\mathrm{gain,cryo}}(400\ \mathrm{MHz})} \approx 2.3 \quad [4]$$

Hence, the expected gain under approximated optimal conditions for the ^{13}C CryoProbe™ is more than two-fold higher than for the CryoProbe™ at proton frequency. It should be noted that the calculation in Equation [4] and the expected gain represent only a rough estimation.

EXPERIMENTAL METHODS

Coils

We compared a ^{13}C CryoProbe™ for mouse brain imaging (Bruker, Ettlingen, Germany; Fig. 1c) with a standard surface coil from the same vendor (Fig. 1a) and a home-built coil with an optimized geometry for mouse brain imaging (Fig. 1b) on a 9.4-T horizontal-bore animal scanner (Bruker).

The ^{13}C CryoProbe™ consists of an anatomically shaped, circular, cryogenic ^{13}C coil element and a room temperature ^{1}H saddle coil. Both channels operate in transmit/receive mode. As a result of its geometry, only small animals, such as mice, can be scanned (Fig. 1c). The ^{13}C coil as well as the cryogenic preamplifier are encapsulated in an insulated vacuum chamber and are cooled with gaseous helium in a closed-cycle cooling system to lower their operating temperature to approximately 30 K/77 K (coil/preamplifier). The coil area contacting with the animal is heated and actively temperature controlled. Temperatures of 20 and 36 °C were used in the phantom and *in vivo* experiments, respectively.

The standard surface coil (Fig. 1a) consists of a double-tuned, flat, single loop (20 mm in diameter) with manual tuning on both frequencies.

The home-built ^{13}C transceiver surface coil (Fig. 1b) was constructed to resemble optimal coil geometry and approximates the CryoProbe's geometrical design, albeit they are not exactly the same. The detector element was square-shaped from 1mm-thick silver wire insulated by heat shrink with a side length of 18 mm, which was anatomically shaped by bending it on a 15-mm-diameter cylindrical former. Variable tune and match capacitors were part of the circuit design. Localization and shimming were performed using a linear ^{1}H volume resonator which was geometrically decoupled from the surface coil.

Both room temperature coils were connected to a broad-band room temperature preamplifier.

We acknowledge that only partial information regarding the actual coil dimensions of the ^{13}C surface resonator element in the cryogenic coil are available. From the patent [NMR Probehead with heated housing, Haueisen, US Patent

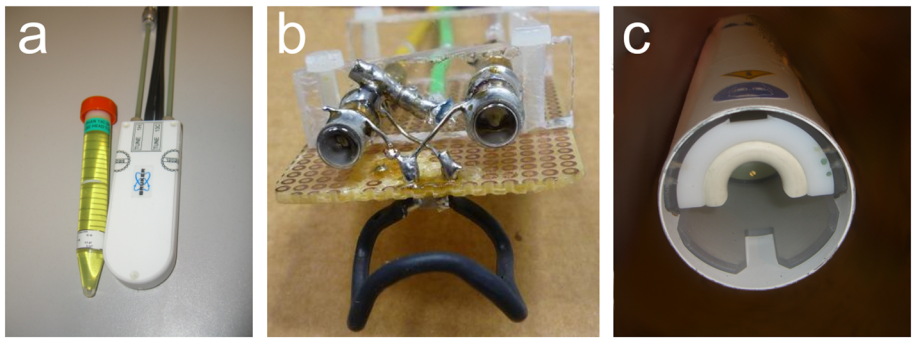

Figure 1. Images of the three coils used in this experiment: (a) standard surface coil and the phantom containing dimethyl sulfoxide (DMSO); (b) home-built ^{13}C transceiver surface coil with anatomically shaped square element; (c) anatomically shaped ^{13}C CryoProbe™ with an additional ^{1}H saddle coil.

Application 2007] and latest review article by the producers (13), it is obvious that a circular slightly anatomically shaped surface coil was used. The exact dimensions remain unknown as they represent proprietary information of the manufacturer.

The dimensions of the cryogenic coil are relatively small, therefore substantially contributing to the benefit from cryogenic cooling (13). Room temperature coils at this small size and low resonance frequency, however, benefit from increased detector inductance as a result, for example, of multi-winding, anatomical shaping and positioning in close sample proximity (14). As described in Elabyad *et al.* (15), the two-turn spiral coil at 18.7 MHz can improve the SNR for diameters of less than 5 cm, whereas cryogenic cooling did not benefit from the multi-turn approach. Hence, the optimum cryogenic and room temperature coil geometry at 100 MHz can differ for the same application; i.e. for mouse brain ^{13}C NMR.

Quality factor (*Q*-factor) measurements

The *Q*-factor was measured for each coil when loaded with a phantom and in the unloaded condition. A 15-mL tube filled with 5 mL of dimethyl sulfoxide (DMSO), 10 mL of distilled water and NaCl (4.3 g/L) was used as a phantom (Fig. 1a). According to Darrasse and Kassab (16), one can assess the coil sensitivity using two geometrically decoupled pick-up loops (dual-loop probe). We used such a dual-loop probe, where each of the loops had a diameter of 4 mm. The dual-loop probe was connected to a vector network analyzer (DG8SAQ USB-Controlled VNWA 3, SDR-Kits, Trowbridge, Wiltshire, UK) and a transmission measurement (s_{21}) was recorded. The *Q*-factor of the resonator under test was computed from the bandwidth (BW) $\Delta\omega$ of –3 dB and the center frequency ω_0, as follows:

$$Q = \frac{\omega_0}{\Delta\omega} \quad [5]$$

The theoretically expected SNR benefit of the cryogenic coil over the room temperature coils was computed according to equation [8] in Junge (13):

$$Q_{\text{sample}}^{-1} = Q_{\text{loaded}}^{-1} - Q_{\text{unloaded}}^{-1} \quad [6]$$

and

$$\frac{\text{SNR}_{\text{LT}}}{\text{SNR}_{\text{RT}}} = \frac{\sqrt{T_{\text{RT}}/Q_{\text{unl,RT}} + T_{\text{sample}}/Q_{\text{sample,RT}}}}{\sqrt{T_{\text{LT}}/Q_{\text{unl,LT}} + T_{\text{sample}}/Q_{\text{sample,LT}}}} \quad [7]$$

where the subscripts 'LT' and 'RT' represent the low and room temperature resonators, respectively, T is the coil temperature and T_{sample} is the sample temperature.

Phantom measurement

In phantom measurements, we used the same DMSO phantom as described previously. After first- and second-order shimming on the proton channel and calibration of the ^{13}C transmitter to obtain the maximum signal, we acquired a spectrum from a $7 \times 6 \times 10$-mm^3 voxel using an image-selected *in vivo* spectroscopy (ISIS) localization sequence. ISIS consisted of adiabatic slice-selective refocusing pulses and a rectangular excitation pulse; 16 averages (128 total acquisitions) were obtained in each experiment with an acquisition time of 1360 ms (8192 acquisition points) and TR of 10 s. The voxel was placed 1.6 mm from the phantom's edge to mimic an *in vivo* voxel location. The B_0 field was optimized with field map-based shimming ('Mapshim', Bruker) over a $10 \times 10 \times 10$-mm^3 voxel and yielded a full width at half-maximum (FWHM) smaller than 4 Hz in all three experiments.

In addition, we obtained a three-dimensional CSI from the same phantom after global first- and second-order shimming. The CSI consisted of four averages with TR = 800 ms (total scan time, 20 min), a 30° flip angle, field of view of $25 \times 25 \times 50$ mm^3 and a matrix of $8 \times 8 \times 16$, leading to a nominal isotropic voxel size of 3.125 mm^3. An acquisition time of 629 ms (4096 acquisition points) was used.

To avoid additional noise originating from the corresponding ^{1}H coils, all phantom measurements were conducted without spectroscopic decoupling. The ^{1}H coils were only in use for imaging and B_0 field optimization.

Animal experiment

To allow for direct comparison, *in vivo* ^{13}C spectra were acquired twice on the same C57/Bl6 mouse (33 g) during the administration of ^{13}C-enriched glucose using first the ^{13}C CryoProbe™ and, after 1 week of recovery, the standard surface coil. After each measurement, the injection site was inspected carefully for any signs of suboptimal ^{13}C administration (swollen tail or visible leakage of glucose solution). Two weeks after the last injection, the animal had no discoverable injuries at the tail. This experiment was approved by the Committee on Animal Care and Use (Regierungspräsidium Karlsruhe, Germany), and was carried out in accordance with the local Animal Welfare Act and the European Communities Council Directive of 24 November 1986 (86/609/EEC).

The freely breathing mouse was anesthetized with isoflurane (1–1.5%), and [1-^{13}C]-enriched glucose (20% w/v solution) was administered through the tail vein. We used an infusion protocol with an exponentially decaying bolus in the first 5 min (99%-enriched glucose), followed by a continuous 70%-enriched infusion of 0.33 mL/h over 4 h, adapted from ref. (5,17), which resulted in sustained hyperglycemia during the whole experiment.

In order to acquire localized mouse brain spectra, we used ISIS in both *in vivo* experiments. Based on ^{1}H anatomical images, the voxel ($6 \times 5.5 \times 4\ mm^3$) was placed at the same position within the mouse brain in both experiments. After localized first- and second-order shimming using 'Fastmap' (18) (cube size, $5.5 \times 5.5 \times 5.5\ mm^3$), FWHMs for the water signal of 28 and 27 Hz were achieved in the CryoProbe™ and standard coil experiment, respectively.

ISIS consisted of adiabatic inversion pulses with a BW of 220 ppm and a 90° rectangular pulse ($BW_{90} = 254$ ppm) for the CryoProbe™ experiment and BW_{180} of 63 ppm and BW_{90} of 84 ppm for the standard coil. Proton-decoupled (WALTZ16, 200-μs elements, center frequency at 3 ppm during the first 60% of the acquisition time) spectra were acquired with 112 averages and TR = 3 s, resulting in a time resolution of 6 min per spectrum (including one ISIS dummy cycle) over 240 min with a center frequency at 38.9 ppm. The acquisition time was 406.32 ms with a dwell time of 49.6 μs (4096 points) and a BW of 100.14 ppm for both experiments.

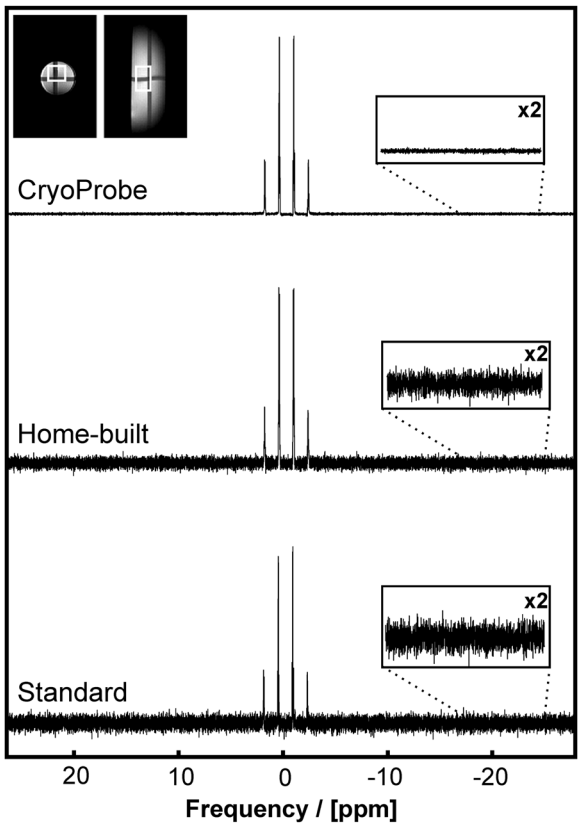

Figure 2. Spectra obtained from single-voxel phantom measurements and scaled for the purpose of all spectra to have a similar intensity. From top to bottom: ^{13}C CryoProbe™, home-built transceiver coil and standard surface coil. Top left: location of the voxel ($7 \times 6 \times 10\ mm^3$). The voxel was placed 1.6 mm from the edge of the phantom containing dimethyl sulfoxide (DMSO).

RESULTS

Q-factor measurements

The mean and standard deviation of three loaded and unloaded *Q*-factor measurements for each coil and the estimated theoretical SNR gain neglecting geometrical detector variations are listed in Table 1. The SNR gain was calculated according to Equations [6] and [7] using $T_{RT} = 293$ K, $T_{sample} = 293$ K and $T_{LT} = 30$ K. The highest *Q*-factor was clearly determined for the cryogenic coil, whereas, for the two room temperature coils, the home-built resonator performed better than the commercially available resonator (Table 1).

Phantom measurements

SNRs of the localized single-voxel phantom measurements were calculated in the jMRUI package (19) (version 4) using AMARES (20), which performs a time-domain fitting. We used 16 Lorentzian peaks to fit the real part spectra, which accounts for possible differences in shimming results. Noise was calculated from the last 812 points of the free induction decay, yielding an SNR of 140 for the CryoProbe™. The standard surface coil and home-built coil reached SNRs of 14.1 and 34.8, respectively. Thus, the SNR enhancement was approximately four for the best available room temperature resonator in these phantom measurements (Fig. 2).

The CSI images obtained from the three coils were reconstructed to a $12 \times 12 \times 24$ matrix and each spectrum was zero filled with 16 K points (Fig. 3) using MATLAB 8.1 (The MathWorks, Inc., Natick, MA, USA). To determine the SNR in each voxel, we calculated the mean of the absolute spectrum in a frequency range covering the whole DMSO quartet, adjusted for each experiment, divided by the root-mean-square of the same frequency range placed 10 ppm to the left of the DMSO quartet. Similarly to the single-voxel experiment, this method also accounts for possible differences in shimming results of the three experiments. Figure 3a demonstrates the locally dependent SNR distribution of the three surface coils. While the standard coil shows a typical field of view of a flat resonator, the fields of view of the CryoProbe™ and home-built coil are more comparable because of the similar anatomical shape, with a slightly higher homogeneity at the bottom of the phantom for the home-built coil. As the three-dimensional CSI had to be planned on the basis of the ^{1}H images, the actual gain in SNR was calculated within the respective axial slice containing the highest SNR value for each coil. This leads to maximum SNR ratios of factors 5

Table 1. Measured quality factors (*Q*-factors) (mean ± standard deviation) in loaded [dimethyl sulfoxide (DMSO) phantom] and unloaded conditions. The signal-to-noise ratio (SNR) gains (SNR_{LT}/SNR_{RT}) were calculated according to Equations [6] and [7] using $T_{RT} = 293$ K, $T_{sample} = 293$ K and $T_{LT} = 30$ K

	$Q_{unloaded}$	Q_{loaded}	SNR_{LT}/SNR_{RT}
CryoProbe™	353 ± 0.01	302.5 ± 1.75	–
Room temperature home-built	259 ± 2.2	145 ± 2.5	3
Room temperature standard	109 ± 0.6	108 ± 0.6	3.5

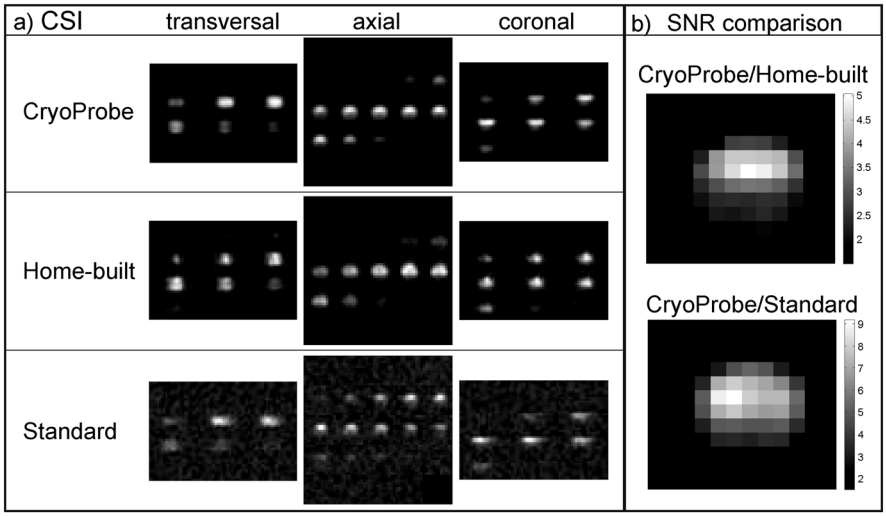

Figure 3. (a) Chemical shift images obtained from a dimethyl sulfoxide (DMSO) phantom after a scan time of 20 min. (b) Signal-to-noise ratio (SNR) gain of the CryoProbe™ compared with the home-built coil and standard planar resonator. The respective axial slices containing the highest SNR values are compared.

and 9.2 for the CryoProbe™ compared with the home-built and standard coils, respectively (Fig. 3b). The mean of the ten voxels with the highest SNR in the three-dimensional images yields SNRs of 13.8, 2.8 and 1.8 for the CryoProbe™, home-built resonator and standard coil, respectively.

Animal experiment

The time evolution of label incorporation over the whole CryoProbe™ measurement is illustrated in Fig. 4. Although the SNR of the CryoProbe™ is sufficient to detect GABAC2 and GABAC4, the spectra acquired with the standard coil hardly show any signal above noise level. Thus, we chose to sum the last 15 measurements of each experiment to obtain spectra with sufficient SNR for a comparison. As the same mouse was measured twice using exactly the same infusion protocol, this approach should lead to reliable results.

The respective voxel location of both measurements and the absolute spectra of the summed last 15 acquisitions are presented in Fig. 5. As a result of the poor spectral quality of the standard coil measurement, a 5-Hz apodization was applied to both spectra. After a high zero filling of 64 K points, a Lorentzian was fitted to the highest signal in the real part spectrum between 25 and 60 ppm, which was glutamine C4 in both experiments. Noise was calculated as the root-mean-square of the real part spectrum in the region between –10 and 0 ppm, a range which can be considered as pure noise. These calculations performed in MATLAB 8.1 lead to a gain in SNR of about nine for the CryoProbe™. However, because of the poor performance of the standard coil, this value should be considered as a rough estimate.

DISCUSSION

The home-built resonator was constructed to resemble close to optimized coil geometry for room temperature coils in order to acquire NMR signals from mouse brain. To increase the detector inductance, a square base shape of the coil was chosen with slightly larger dimensions compared with the CryoProbe™. Although a volume coil can increase the filling factor, it is known that the SNR per voxel is higher for surface coils, thus providing sufficient penetration depth (21). The clear SNR improvement compared with the commercial standard room temperature resonator is evident herein presented from phantom tests.

In a previous study (9), using a ^{1}H CryoProbe™ at 200 MHz, providing similar dimensions for mouse brain MRI, the *Q*-factor at cryogenic temperature was reported to be 332/286 = $Q_{unloaded}/Q_{loaded}$(DMSO), whereas the results changed when the same resonator was operated at room temperature

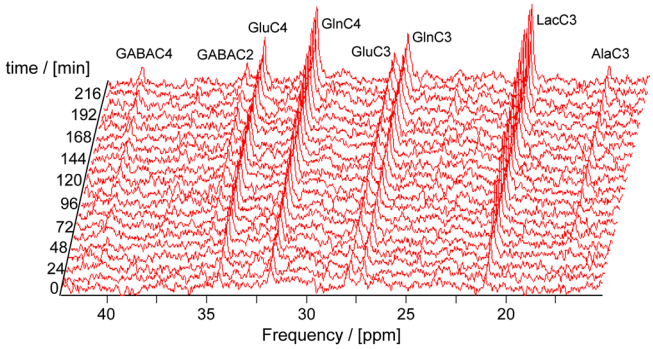

Figure 4. Time course of label incorporation during the *in vivo* CryoProbe™ experiment. Two successive spectra were summed resulting in 12-min spectra. Ala, alanine; GABA, γ-aminobutyric acid; Gln, glutamine; Glu, glutamate; Lac, lactate; the appendices C2, C3, and C4 indicate the respective carbon positions.

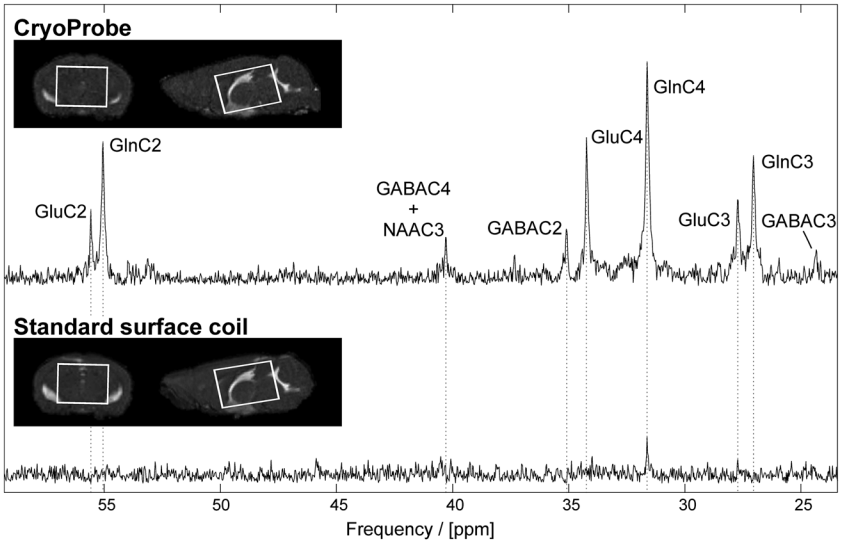

Figure 5. Absolute spectra (5-Hz apodization) of the summed last 15 measurements acquired using the CryoProbe™ (top) and the standard surface coil (bottom). Top left: respective voxel location. GABA, γ-aminobutyric acid; Gln, glutamine; Glu, glutamate; NAA, N-acetylaspartate; the appendices C2, C3, and C4 indicate the respective carbon positions.

to 148/136 = $Q_{unloaded}/Q_{loaded}$(DMSO). The *Q*-factor values measured in this study for the three resonators used correspond well with these measurements (CryoProbe™, 353/302 = $Q_{unloaded}/Q_{loaded}$; home-built room temperature coil, 259/145 = $Q_{unloaded}/Q_{loaded}$). Baltes *et al*. (10) reported no *Q*-factors for the 400-MHz coil and Junge (13) reported much higher *Q*-factors for a 7-mm-diameter coil; however, it remains unclear whether these values were measured or simulated.

The *Q*-factor achieved using the home-built coil in loaded and unloaded conditions demonstrated a large difference, indicating large sample losses, which can be attributed to the fact that the coil was placed in close proximity to the sample. Placing a cryogenic coil in similar close proximity to the sample is impossible because of the high temperature gradient that must be catered for between both the coil and the sample.

The dual-loop probe method for estimation of the *Q*-factor only takes into account the effect of the resonant loop circuit, thus neglecting the influence of losses occurring in the residual electronic components (e.g. radiofrequency coaxial cable, preamplifier). Furthermore, the equations given by Junge (13) are suitable for coils of similar dimensions. Indeed, the room temperature coils clearly had different dimensions compared with the cryogenic coil. This, in turn, was necessary to test the best available coil solution for users with and without access to custom-built room-temperature coils. In addition, the given equations neglect different distances from the coil to the sample, which varied with the lowest distance provided by the home-built surface coil.

The single-voxel phantom measurements yielded an SNR gain by a factor of about 10 compared with the standard surface single-loop room temperature coil ($SNR_{cryo}/SNR_{standard}$ = 140/14.1). The *in vivo* comparison resulted in a gain of about nine which is in line with the phantom experiment, but should nevertheless be regarded as a rough estimation. In comparison with the home-built coil with a more ideal anatomical coil design, an SNR gain of four was observed in the single-voxel phantom experiments ($SNR_{cryo}/SNR_{home\text{-}built}$ = 140/34.8). Ratering *et al*. (9) found an SNR gain of 2.47 ± 0.01 for a ^{1}H CryoProbe™ compared with a geometrically similar room temperature coil in a low-conductivity DMSO phantom. Baltes *et al*. (10) obtained average gains in SNR of 2.40 and 2.42 in phantom measurements using a ^{1}H CryoProbe™. In conjunction with the approximated SNR gain improvement calculated in the 'Theory' section of about 2.3 for a cryogenic coil at carbon frequency compared with one at proton frequency, the SNR gain of four in the single-voxel experiment for the ^{13}C CryoProbe™, in comparison with the home-built coil, is in the expected range.

A fair approach to compare the sensitivity amongst coils with different diameters seems to be to acquire CSIs for each coil, ensuring that the flip angle is similar amongst coils. Then, the truly achieved sensitivity gain in a certain distance from the coil can be compared, as has been demonstrated for spin-echo and gradient-echo images for a ^{1}H cryo-mouse coil (9,10). Despite the low spatial resolution compared with that achieved in ^{1}H images, the CSI measurements presented here reflect the effects of the different coil designs in relation to field of view and B_1 homogeneity. Although the estimation of the locally dependent SNR values of the three coils in a general approach is difficult and clearly depends on the designated purpose, the highest gain for the CryoProbe™ is achieved in the area around the top of the phantom to its center, covering a range of approximately 6–8 mm (as demonstrated in Fig. 3b). Translated to *in vivo* experiments, this range would cover a mouse brain, and supports the findings in the single-voxel phantom and *in vivo* measurements.

In addition, our study shows that the cryo-technique enables the localized determination of dynamic metabolite rates in mouse brain via ^{13}C MRS. The results of the *in vivo* experiment exhibit a high SNR at a relatively high temporal resolution. Despite the small voxel size of 132 μL, a considerably broad FWHM of 28 Hz and the use of only [1-^{13}C]-enriched glucose, without application of polarization transfer techniques, the SNR was sufficiently high to detect the label incorporation of the most important metabolites. Even the detection of GABA (C4 and C2 position) was possible in a 6-min scan, which would allow a GABAergic compartment to be taken into account in metabolic models in future studies.

These results can be compared with the dynamic ^{13}C NMR measurements in mice at 7 T using an elliptical surface room temperature coil by Nabuurs *et al*. (2). In this study, comparable water linewidths of 27–30 Hz were achieved; however, the

authors followed a fundamentally different approach. First, a 99%-enriched [1,6-$^{13}C_2$]-glucose infusion was selected, which doubles the fractional enrichment compared with [1-^{13}C]-glucose (4). Second, the voxel location was similar but larger in size (175 μL compared with 132 μL), which compensates for the higher magnetic field strength in our experiment. Third, they used a different NMR sequence including semi-adiabatic distortionless enhanced polarization transfer, which would theoretically result in a four-fold higher signal. Nevertheless, the spectrum presented here summed over the last 1.5 h is at least on a par with, if not better than, that presented by Nabuurs *et al*. (2) obtained during the last hour of a 4-h glucose experiment. Considering all these factors, the CryoProbe™ would have an assumed SNR improvement of about 6.5. While the authors concluded that dynamic *in vivo* ^{13}C MRS on mouse brain is feasible using [1,6-$^{13}C_2$]-glucose in combination with localized distortionless enhanced polarization transfer, we suggest that, when using a CryoProbe™, it would even be feasible using [1-^{13}C]-glucose and no polarization transfer.

Moreover, because of the high efficiency of the cryogenic coil, the use of the CryoProbe™ enables the application of comparably short radiofrequency pulses and thus the BW of the signal excitation can be increased, i.e. the acquisition of a wider range of resonances in a single experiment becomes achievable. Overall, this SNR gain allows considerably shorter acquisition times and higher spatial resolution. Taken together, the use of a ^{13}C CryoProbe™ enables the localized *in vivo* investigation of metabolism within mouse brain with high accuracy, and thus paves the way to translational studies of altered brain metabolism in mouse models and humans.

Acknowledgements

The authors thank T. Wokrina (Bruker BioSpin AG, Ettlingen, Germany), D. Marek (Bruker BioSpin AG, Fällanden, Switzerland) and B. Lanz (LIFMET CIBM, EPFL, Lausanne, Switzerland) for their support. This work was supported by the "Deutsche Forschungsgemeinschaft" (DFG) through a center grant to G. E. (SFB636, project Z03).

REFERENCES

1. Gruetter R, Adriany G, Choi IY, Henry PG, Lei H, Oz G. Localized in vivo ^{13}C NMR spectroscopy of the brain. NMR Biomed. 2003; 16: 313–338.
2. Nabuurs CI, Klomp DW, Veltien A, Kan HE, Heerschap A. Localized sensitivity enhanced in vivo ^{13}C MRS to detect glucose metabolism in the mouse brain. Magn. Reson. Med. 2008; 59: 626–630.
3. Henry PG, Adriany G, Deelchand D, Gruetter R, Marjanska M, Oz G, Seaquist ER, Shestov A, Ugurbil K. In vivo ^{13}C NMR spectroscopy and metabolic modeling in the brain: a practical perspective. Magn. Reson. Imaging, 2006; 24: 527–539.
4. de Graaf RA, Brown PB, Mason GF, Rothman DL, Behar KL. Detection of [1,6-$^{13}C_2$]-glucose metabolism in rat brain by in vivo ^{1}H-[^{13}C]-NMR spectroscopy. Magn. Reson. Med. 2003; 49: 37–46.
5. Duarte JM, Lanz B, Gruetter R. Compartmentalized cerebral metabolism of [1,6-(13)C]glucose determined by in vivo (13)C NMR spectroscopy at 14.1 T. Front. Neuroenergetics 2011; 3: 3.
6. Gruetter R, Seaquist ER, Ugurbil K. A mathematical model of compartmentalized neurotransmitter metabolism in the human brain. Am. J. Physiol. Endocrinol. Metab. 2001; 281: E100–E112.
7. van Eijsden P, Behar KL, Mason GF, Braun KP, de Graaf RA. In vivo neurochemical profiling of rat brain by ^{1}H-[^{13}C] NMR spectroscopy: cerebral energetics and glutamatergic/GABAergic neurotransmission. J. Neurochem. 2010; 112: 24–33.
8. Darrasse L, Ginefri JC. Perspectives with cryogenic RF probes in biomedical MRI. Biochimie 2003; 85: 915–937.
9. Ratering D, Baltes C, Nordmeyer-Massner J, Marek D, Rudin M. Performance of a 200-MHz cryogenic RF probe designed for MRI and MRS of the murine brain. Magn. Reson. Med. 2008; 59: 1440–1447.
10. Baltes C, Radzwill N, Bosshard S, Marek D, Rudin M. Micro MRI of the mouse brain using a novel 400 MHz cryogenic quadrature RF probe. NMR Biomed. 2009; 22: 834–842.
11. Griffin JL, Keun H, Richter C, Moskau D, Rae C, Nicholson JK. Compartmentation of metabolism probed by [2-^{13}C]alanine: improved ^{13}C NMR sensitivity using a CryoProbe™ detects evidence of a glial metabolon. Neurochem. Int. 2003; 42: 93–99.
12. Ginefri JC, Darrasse L, Crozat P. High-temperature superconducting surface coil for in vivo microimaging of the human skin. Magn. Reson. Med. 2001; 45: 376–382.
13. Junge S. *Cryogenic and Superconducting Coils for MRI*. eMagRes, 2007. DOI: 10.1002/9780470034590.emrstm1162
14. Wetterling F, Högler M, Molkenthin U, Junge S, Gallagher L, Mhairi Macrae I, Fagan AJ. The design of a double-tuned two-port surface resonator and its application to in vivo hydrogen- and sodium-MRI. J. Magn. Reson. 2012; 217: 10–18.
15. Elabyad IA, Kalayciyan R, Wetterling F, Schad LR. Enhancing the detector sensitivity of a radio frequency surface resonator for potassium-39 MRI at 18.7 MHz: probing different geometries at various temperatures. *42nd European Microwave Conference (EuMC),* Amsterdam, the Netherlands, 2012; 444–447.
16. Darrasse L, Kassab G. Quick measurement of NMR-coil sensitivity with a dual-loop probe. Rev. Sci. Instrum. 1993; 64: 1841.
17. Henry PG, Tkac I, Gruetter R. ^{1}H-localized broadband ^{13}C NMR spectroscopy of the rat brain in vivo at 9.4 T. Magn. Reson. Med. 2003; 50: 684–692.
18. Gruetter R. Automatic, localized in vivo adjustment of all first- and second-order shim coils. Magn. Reson. Med. 1993; 29: 804–811.
19. Vanhamme L, van den Boogaart A, Van Huffel S. Improved method for accurate and efficient quantification of MRS data with use of prior knowledge. J. Magn. Reson. 1997; 129: 35–43.
20. Vanhamme L, Van Huffel S, Van Hecke P, van Ormondt D. Time-domain quantification of series of biomedical magnetic resonance spectroscopy signals. J. Magn. Reson. 1999; 140: 120–130.
21. Mispelter J, Lupu M, Briguet A. *NMR Probeheads for Biophysical and Biomedical Experiments: Theoretical Principles and Practical Guidelines*. Imperial College Press: London, 2006.